

Proteomic Characterization of the Dynamics of Ischemic Stroke in Mice

Rong-Fang Gu, Terry Fang, Ashley Nelson, Stefka Gyoneva, Benbo Gao, Joe Hedde, Kate Henry, Emily Peterson, Linda C. Burkly,* and Ru Wei*



Cite This: *J. Proteome Res.* 2021, 20, 3689–3700



Read Online

ACCESS |



Metrics & More



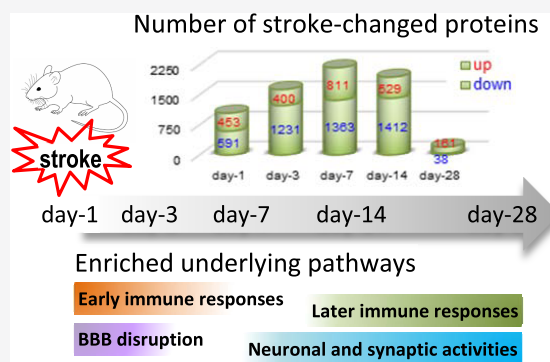
Article Recommendations



Supporting Information

ABSTRACT: Novel therapies and biomarkers are needed for the treatment of acute ischemic stroke (AIS). This study aimed to provide comprehensive insights into the dynamic proteome changes and underlying molecular mechanisms post-ischemic stroke. TMT-coupled proteomic analysis was conducted on mouse brain cortex tissue from five time points up to 4 weeks poststroke in the distal hypoxic-middle cerebral artery occlusion (DH-MCAO) model. We found that nearly half of the detected proteome was altered following stroke, but only ~8.6% of the changes were at relatively large scales. Clustering on the changed proteome defined four distinct expression patterns characterized by temporal and quantitative changes in innate and adaptive immune response pathways and cytoskeletal and neuronal remodeling. Further analysis on a subset of 309 “top hits”, which temporally responded to stroke with relatively large and sustained changes, revealed that they were mostly secreted proteins, highly correlated to different cortical cytokines, and thereby potential pharmacodynamic biomarker candidates for inflammation-targeting therapies. Closer examination of the top enriched neurophysiologic pathways identified 57 proteins potentially associated with poststroke recovery. Altogether, our study generated a rich dataset with candidate proteins worthy of further validation as biomarkers and/or therapeutic targets for stroke. The proteomics data are available in the PRIDE Archive with identifier PXD025077.

KEYWORDS: stroke, acute ischemic stroke (AIS), MCAO, DH-MCAO, proteomics, tandem mass tags (TMT), immune response, inflammation, stroke recovery, stroke biomarkers



INTRODUCTION

Acute ischemic stroke (AIS) is the second leading cause of death worldwide and over half of affected patients suffer persistent long-term disability from the neurologic injury.¹ Only one drug, recombinant tissue plasminogen activator (tPA), is approved for treating AIS, and it must be administered within a few hours. A deeper understanding of the pathophysiological mechanisms underlying stroke would enable the identification of targets and development of therapeutics to prevent further brain injury and facilitate neurological recovery, as well as biomarker discovery to improve diagnosis, guide treatment, and monitor response to therapy. Animal models are essential tools in these activities. The distal hypoxic-middle cerebral artery occlusion (DH-MCAO) model features permanent occlusion at the distal middle cerebral artery, followed by 1 h of hypoxia, which results in reliable and reproducible infarcts, neuroplasticity changes, and behavioral deficits.^{2–4} Moreover, the permanent nature of the artery occlusion may better mimic human stroke, in which revascularization is rare.² DH-MCAO is thus advantageous for assessments of therapeutic strategies.

Several proteomic analyses of AIS using MCAO models^{5–9} have been reported. They were conducted on transient MCAO

mouse or rat models and generally focused on the acute phase poststroke. Law et al.¹⁰ also used a transient model but evaluated differentiated recovery of eight cynomolgus monkeys at 28 days after MCAO-induced stroke. To our knowledge, no proteomic analysis of AIS using a permanent MCAO occlusion model has been reported. This study aimed to characterize the longitudinal proteomic changes caused by ischemic stroke using the DH-MCAO mouse model.

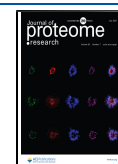
EXPERIMENTAL PROCEDURES

Study Design

The proteomics study was carried out using 45 male mice (C57Bl/6, 16-week old), divided into five groups. Each group contained nine mice, six of which underwent MCAO surgery

Received: March 31, 2021

Published: June 4, 2021



(stroke mice) and three underwent sham surgery, i.e., the same surgical procedure but without cauterization of the MCA. All stroke or sham mice were followed by 1 h hypoxia treatment. The five groups of animals were sacrificed on day 1, 3, 7, 14, and 28, respectively, after surgery and hypoxia treatment to capture both initial injury and recovery processes. At each time point, brain cortex tissues were collected from both ipsilateral and contralateral hemispheres of stroke mice (2 samples per mouse) and from ipsilateral hemispheres of sham mice (1 sample per mouse), resulting in 15 tissue samples in each group (time point): 6 biological replicates of stroke ipsilateral, 6 biological replicates of stroke contralateral, and 3 biological replicates of sham ipsilateral, hereafter referred to as “strk_Ip”, “strk_Ct”, and “sham_Ip”, respectively.

To fit tandem mass tag (TMT) 10-plex labeling design, 70 tissue samples were used in this study: all 15 samples collected on days 1, 3, 7, and 14, and 10 samples collected on day 28 (4 strk_Ip, 4 strk_Ct, and 2 sham_Ip). Additionally, plasma samples were collected from all mice at corresponding time points for cytokine measurements.

DH-MCAO Sample Generation

All experimental procedures using mice were approved by the Biogen Institutional Animal Care and Use Committee (IACUC). Male, 16-week old, C57BL/6J mice were used for this study. Throughout the duration of this study, water and chow were provided to mice ad libitum.

All mice were subjected to MCAO or sham surgery as described by Doyle et al.,⁴ followed by 1 h hypoxia treatment [see details in the [Supplementary Methods](#), Supporting Information (SI)]. At the end of the hour in hypoxia, mice were returned to their home cage. At either 1, 3, 7, 14, or 28 days post-surgery and hypoxia treatment, mice were humanely euthanized in a CO₂ chamber. Blood was collected via cardiac puncture into K₂EDTA tubes and stored on ice. Within 0.5–1 h of collection, the blood samples were centrifuged at 3000g for 5 min at 4 °C, and plasma was separated, aliquoted, and stored at –80 °C until analysis. Mice were subsequently transcatheterially perfused with cold PBS. Brains were removed and dissected to obtain both the infarcted region on the ipsilateral cortex and a corresponding area of tissue on the contralateral cortex. All tissues were snap-frozen and stored at –80 °C until processing.

Tissue Processing and Cytokine and Albumin Analysis

Brain cortical tissue was homogenized with metal beads in 20× volume to weight (e.g., 200 µL for 10 mg) using cold 1× Tris buffer (25 mM, pH 7.4) with cOmplete Mini protease inhibitor tablets (1 tablet per 10 mL of buffer). Homogenized samples were centrifuged at 1000g for 10 min at 4 °C to generate supernatant (S1) for proteomic analysis. The S1 supernatant was further centrifuged at 6000g for 1 h at 4 °C to generate supernatant (S2) for cytokine and albumin analysis. Protein concentration of the S2 supernatant was determined with the BCA assay, and samples were next normalized to 1.5 mg/mL protein concentration.

For cytokine analysis, brain S2 supernatants (1.5 mg/mL) and plasma samples were diluted in Diluent 41 at 1:4 and 1:20, respectively. Fifty microliters of diluted samples was added to MSD V-plex ELISAs (K15048D, K15245D) and incubated overnight with shaking at 4 °C. Secondary antibody addition and development were performed according to the manufacturer's instructions. Western blot analysis was used to measure albumin concentrations in brain tissue using S2 supernatants (see details in the [Supplementary Methods](#), SI).

Proteomics Tissue Lysis and Protein Digestion

The S1 supernatants were further lysed in ice-cold lysis buffer (8 M urea in 50 mM Tris-HCl, pH 7.4) with protease inhibitor cocktails (Sigma) by sonicating at 150 W for 10 s in 4 °C water bath using an E220 focused-ultrasonicator (Covaris, MA). The lysates were next clarified by centrifuging at 4 °C and 18 000g for 20 min and protein concentrations were measured using the Bradford assay. The protein extracts were subsequently reduced (dithioerythritol, 15 mM, 45 min at 37 °C), alkylated (iodoacetamide, 30 mM, 30 min at room temperature in the dark), and diluted to 1 M urea in 50 mM ammonium bicarbonate followed by tryptic digestion (protein-to-protease ratio at 30:1 w/w) for 16 h at 37 °C.

Tandem Mass Tag (TMT) 10-plex Labeling and Peptide Fractionation

The digests were desalted using C18 StageTip with three-punch C18 mesh (Empore), SpeedVac dried, and stored at –20 °C. Peptide concentrations were measured on a NanoDrop 2000 (Thermo). For each sample, 20 µg of peptides was TMT-labeled according to the vendor's instruction. TMT tags were randomized within each of TMT 10-plex set. The efficiency of the TMT labeling was determined to be greater than 99%. The TMT-labeled samples were then pooled at equal peptide ratios into seven TMT 10-plex sets ([Supplementary Methods](#), Table S1, SI), followed by vacuum centrifugation to near dryness. Subsequently, the resulting peptide mixtures were each high-pH fractionated and concatenated into 12 fractions of similar complexities, resulting in 84 subsamples. The peptides were desalted using C18 StageTip, SpeedVac dried, and kept at –20 °C until nanoLC–MS/MS analysis. The detailed labeling procedure and fractionation steps are provided in the [Supplementary Methods](#) (SI). To obtain relatively homogeneous proteomes among seven TMT 10-plex sets, we assumed that day 1 and 3 samples have relatively similar proteomes, as do those of day 7 and 14; thus, day 1 and 7 samples were pooled in three sets, day 3 and 14 samples were pooled in three sets, and day 28 samples were one set.

nanoLC–MS/MS Analysis

Prior to analysis, the peptide fractions were reconstituted in 2% acetonitrile/0.2% formic acid and analyzed on a nanoLC–MS/MS platform composed of an EASY nLC 1200 coupled to a Q Exactive HF mass spectrometer (Thermo). Peptides were separated on a Thermo EASY-Spray C18 column (50 cm × 75 µm, 2 µm) over a 120 min effective gradient at a flow rate of 275 nL/min. Mass spectrometric data were acquired at data-dependent acquisition mode with a scan range of 200 to 2000 *m/z*, and the top 10 peptide ions were subjected to MS². A 60 000 resolution with 3e6 AGC and 20 ms Maximum IT was set for MS¹, and a 60 000 resolution with 1e6 AGC and 120 ms Maximum IT was set for MS². The isolation window was set to 0.7 Th, an NCE of 33% was used, and the first mass was fixed at 100 *m/z*. In addition, unassigned and singly or >7+ charged species were excluded from MS² analysis, and the dynamic exclusion was set to 30 s.

The mass spectrometric data were searched using MaxQuant (version 1.5.3.8) against the Swiss-Prot mouse database (UniProtKB Release 2016_04) with cysteine carbamidomethylation as a fixed modification and methionine oxidation and protein N-term acetylation as variable modifications. A mass error of 20 ppm and up to two miscleavages were allowed. The false discovery rates (FDRs) at the protein and peptide levels were both set at 1%.

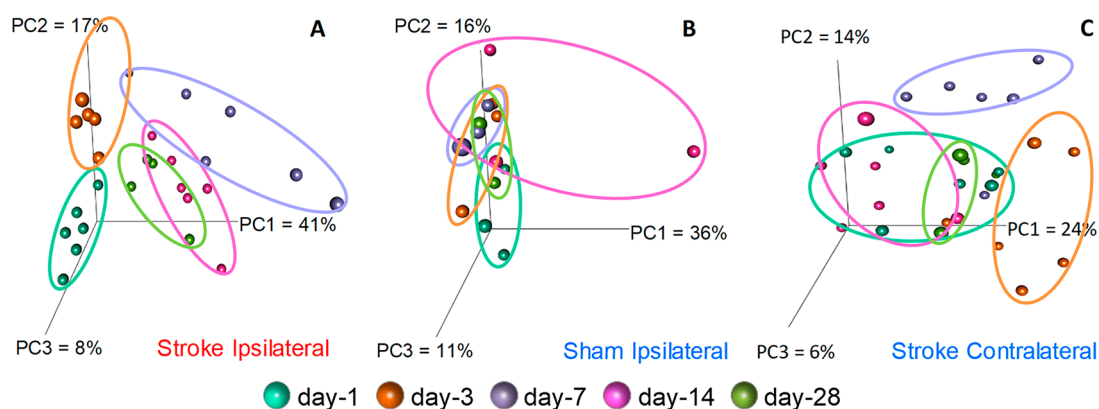


Figure 1. Stroke-induced temporal proteome shift. Principal component analysis of proteomes of day 1 (turquoise), day 3 (orange), day 7 (purple), day 14 (pink) and day 28 (green) in (A) stroke ipsilateral (strk_Ip), (B) sham ipsilateral (sham_Ip), and (C) stroke contralateral (strk_Ct) samples. The ovals are for better visualization.

Data Analysis

Protein lists exported from MaxQuant were used for statistical analysis. The data normalization, principal component analysis (PCA) of proteomes, *K*-means clustering analysis on significantly changed proteins, Pearson correlation and hierarchical clustering between proteomics and biochemical readouts of cytokines and albumin, and statistical analysis of proteomics data were performed using R (version 3.6.1, www.r-project.org). The raw data were normalized to the median intensity of all proteins within each TMT 10-plex set. The normalized intensity for each protein was then transformed to a relative ratio by dividing by the mean normalized intensity of the protein, achieving the mean value of 1 for each protein across all TMT sets. The proteins detected in at least 30% of samples were included in statistical analysis that was performed using the LIMMA package. The *p*-values were adjusted for multiple comparisons using the Benjamini–Hochberg (BH) method. A protein was considered significantly different between groups if it had a BH-adjusted *p*-value <0.05. Only strk_Ip and sham_Ip data, which are most relevant to plasma cytokine measurement, were used in the correlation analysis. Correlation was considered as weak, moderate, or high when the correlation coefficient (*r*) is 0.33–0.5, 0.5–0.75, or >0.75, respectively. The relevant number of *K*-mean clusters was defined using NbClust (R package). Pathway enrichment analysis was conducted using MetaCore (Clarivate Analytics, version 20.3.70200) with *p* < 0.05 and FDR < 0.05 as a cutoff. A resulting enriched pathway for the changed-protein clusters (see results section later) was considered to be due to detection bias if the FDR-based enrichment ranking was the same as or lower than the enrichment from using the detected proteome (7318 proteins).

Data Availability

The mass spectrometry proteomics data have been deposited to the PRIDE Archive (<http://www.ebi.ac.uk/pride/archive/>) via the PRIDE partner repository with the data set identifier PXD025077.

RESULTS AND DISCUSSION

Proteomic analysis of a total of 70 samples, comprised of stroke ipsilateral, stroke contralateral control, and sham ipsilateral control samples over a time course of 28 days (collected at days 1, 3, 7, 14 and 28), identified and quantified 7609 protein groups, 7318 of which were detected in at least 30% of samples and included in data analysis (referred hereafter as the detected

proteome). The relative abundances of the quantified proteins, by TMT reporter ions, span more than 5 orders of magnitude, indicating a broad dynamic range in our quantitative measurement. Variation in protein quantitation among biological replicates is relatively low, with a percent coefficient variation (%CV) for the majority of the quantified proteins in stroke or control groups at each time point of less than 15%. It is worthy to note that to enhance performance of the proteomic analysis for identifying proteins changed in stroke, two control groups, ipsilateral samples from the sham animals (sham_Ip) and contralateral samples from the stroke mice (strk_Ct), were used in this study. The TMT-labeling set design was balanced between obtaining confidence in stroke-changed proteins versus control samples and capturing kinetic changes of proteins over the time course.

Stroke-Induced Temporal Proteome Shift

To assess stroke-induced proteome changes over time, we performed principal component analysis (PCA) on the stroke and control samples across the five time points poststroke (days 1, 3, 7, 14, 28). This analysis showed a clear temporal separation of strk_Ip samples over the first 2 weeks, as indicated by PC-1 (41%), PC-2 (17%), and PC-3 (8%), and a slight overlap of the day 14 with the day 28 proteome (Figure 1A). Notably, both day 14 and 28 strk_Ip proteomes have smaller separation from day 1 and 3 as compared to day 7, suggesting potential recovery at the proteome scale starting by day 14. In contrast, there was minimal proteome separation of sham_Ip samples over this time course (Figure 1B), indicative of low biological sample variability and the high quality of the proteomic analysis. Temporal separation of strk_Ct proteomes was observed, but only on days 3 and 7 and at a smaller scale (Figure 1C) as compared to that of strk_Ip samples, consistent with the notion that the contralateral area also exhibits stroke-induced changes, likely at delayed time and smaller scale. We next compared the proteomes of stroke to control samples (strk_Ct or sham_Ip) at each time point. Large separation of the strk_Ip proteome from both strk_Ct and sham_Ip control proteomes, by PC1 (46%–69%), was clearly evident at each time point, and minimal or no separation was observed between the two control proteomes, i.e., strk_Ct and sham_Ip (Figure S1, SI). Most importantly, the PCA revealed large proteome changes in response to stroke, with the largest alteration occurring on day 7.

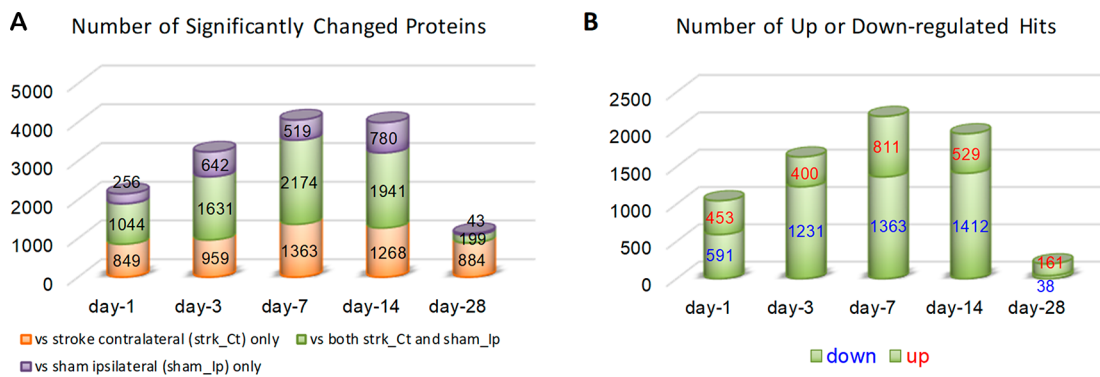


Figure 2. Proteins significantly changed by stroke. (A) Number of significantly changed proteins (adjusted p -value <0.05) vs stroke contralateral (strk_Ct) only (orange), vs sham ipsilateral (sham_Ip) only (purple), and vs both strk_Ct and sham_Ip (green). The overlap in changed proteins using either strk_Ct or sham_Ip control are considered as the hits (green) in this study. (B) Number of up-regulated (red) or down-regulated (blue) proteins among the hits (green bars in A).

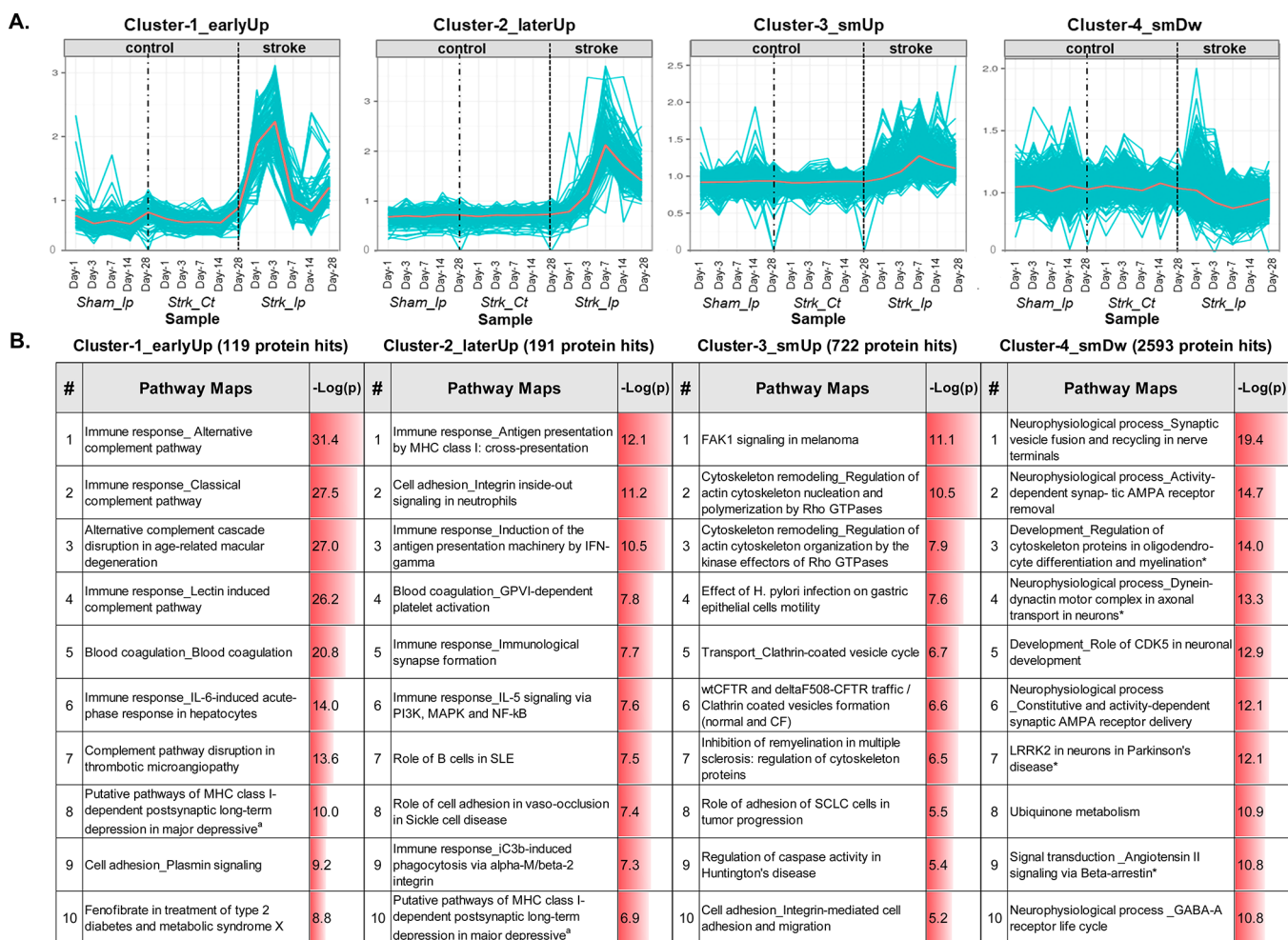





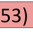





Figure 3. Stroke-induced proteome change patterns and associated pathways. (A) K -mean clusters of 3625 stroke-changed protein hits. Each line represents a pattern of one protein's relative mean expression level across 15 sample groups. Cluster-1_earlyUp: 119 (3.3%) proteins mostly showed a peak on day 3 in strk_Ip with a >2 -fold increase. Cluster-2_laterUp: 191 (5.3%) proteins mostly peaked on day 7 in strk_Ip with a >2 -fold increase. Cluster-3_smUp: 722 (19.9%) proteins mostly peaked on day 7 in strk_Ip with a decrease <1.5 -fold. Note that the fold changes were compared to protein mean expression levels in sham_Ip and/or strk_Ct. (B) Top 10 enriched pathways (FDR <0.05 , ranked by FDR) underlying the four clusters. * indicates that the enrichment is likely due to detection bias (see the methods). ^a indicates that the full pathway name is "Putative pathways of MHC class I-dependent postsynaptic long-term depression in major depressive disorder".

Table 1. Top 309 Proteins as Potential PD Markers and/or Therapeutic Targets for AIS^a

Protein change started on day-1 (115)
Change sustained to ----- day-28 (4) 
Anxa1; C4b; Itih2; Lum
Change sustained to ----- day-14 (10) 
B2m; Cd5l; Cfh; Cfp; Gsn; Itih1; Serpinf1; Vtn; C5ar1; Igkc
Change sustained to ----- day-7 (48) 
Afm; Agt; Ahsg; Alb; Apoc1; Apoh; Azgp1; C8a; C8b; C9; Ces1c; Cfb; Cfi; Cp; Ctla2a; Ecm1; Egfr; F12; F2; Fetub; Fn1; Fstl1; Gc; Gpx3; Hrg; Ica; Igfbp2; Igh-3; Ighg1; Il1rap; Kng1; Mup2; Sepp1; Serpina1a; Serpina1b; Serpina1d; Serpina3k; Serpina3n; Serpina6; Serpincl; Serpind1; Serping1; Tf; Tgfb1; Ttr; Helz; P06330; Pomp
Change sustained to ----- day-3 (53) 
A2m; Ambp; Apcs; Apoa1; Apoa2; Apoa4; C3; C5; C8g; Cd14; Cfd; Chil3; Clec3b; Cpb2; Cpn1; Cpn2; Elane; F13b; Fga; Fgb; Fgg; H2-Q10; Hp; Hpx; Igfbp7; Ighm; Itih4; Klkb1; Lcn2; Lifr; ltf; Mag; Mug1; Mup4; Ngp; Orm1; P01724; P03987-2; Pglyrp1; Plg; Pon1; Rbp4; S100a8; S100a9; Serpina10; Serpina1e; Serpina3m; Serpinf2; Thbs1; P01631; P01646; Kif3c; Prrt2
Protein change started on day-3 (106)
Change sustained to ----- day-28 (44) 
A2mp; Apod; Cd44; Cd63; Cd9; Ctsc; Ctss; Fcgr1g; Fcgr1; Fcgr2; Itgam; Lamp2; Lgals3; Lgals9; Ly86; Lyz2; Plod1; Ptprc; Serpinh1; Clic1; Gfap; Lep1; Plek; Pycard; S100a11; S100a6; Apobr; Arhgdib; Arpc1b; Cagp; Cybb; Dhrs1; Fabp7; Flna; Flnc; Hk2; Msn; Mvp; Plcg2; S100a4; Skap2; Tgm1; Vat1; Vim
Change sustained to ----- day-14 (53) 
Bgn; Cd68; Csf1r; F13a1; Fkbp10; Gusb; H2-D1; Ifi30; Isg15; Lgals1; Lgals3bp; Lgmn; Mrc2; Olfml3; P01864; Tcn2; Trem2; Ugt1a7c; Ybx1; Dab2; Glipr2; Ptbp1; Vamp8; Apbb1ip; Bin2; Bst2; Eif2ak2; Fhl3; Fhod1; Hcls1; Hk3; Ifi204; Iqgap1; Lsp1; Mcm2; Myh9; Ncf1; Nes; Palld; Pld4; Psmb8; Ptrg1; Ptpn6; Rac2; Ripk1; Rrbp1; Sgpl1; Stxbp2; Tagln2; Tes; Tln1; Tmod3; Tpm4
Change sustained to ----- day-7 (9) 
Pros1; Rnase4; Spp1; Stab1; Arg1; Crabp1; Mcm3; Mcm4; Mcm6
Protein change started on day-7 (88)
Change sustained to ----- day-28 (34) 
C1qa; C1qb; C1qc; Cd48; Ctsd; Ctsh; Ctsz; Fbln1; Gpnmb; Grn; Itgb2; Itgb5; Lag3; Lipa; Npc2; Rcn3; Anpep; Anxa4; Ddx58; C2cd3; Fabp4; Fermt3; Gbp2; Ifit2; Ifit3; Inpp5d; Myo1e; Myo1f; Plin2; Renbp; Sash3; Was; Wip1; Zadh2
Change sustained to ----- day-14 (54) 
Apoe; Cd180; Creg1; Ctsa; Ctsb; Fbln1; Gsdmdc1; H2-K1; Hexa; Hexb; Lamp1; Man2b1; Pdia5; Psap; Rnaset2; Scpep1; Siglec1; Tapbp; Aif1; Btk; Erap1; Ftl1; Nfk2; P2rx4; Steap3; Syk; Arhgef6; Ca13; Cotl1; Ctc1; Dtx3l; Fyb; Gbp4; Gpsm3; Hmgcs2; Hmha1; Ifi35; Ifit1; Lpxn; Lrrfip1; Myof; Ncf2; Npl; Ostf1; Parvg; Ppic; Psmb10; Psmb9; Rftn1; Rnf213; Stat1; Uap111; Vav1; Zbp1

^aGene names were used for proteins. The value in parentheses indicates the number of proteins in the category. Red/Blue font indicates that the protein is annotated as “secreted” by UniprotKB subcellular location and/or a signal peptide. Proteins in red font are detected in human plasma according to PPD.

Proteins Significantly Changed by Stroke

We next identified the proteins significantly changed by stroke, namely “hits”, at each time point. We performed two separate data analyses using strk_Ct and sham_Ip as control, respectively. Comparison of strk_Ip and strk_Ct samples generated 1893 (day 1), 2590 (day 3), 3538 (day 7), 3216 (day 14), and 1083 (day 28) hits, while strk_Ip and sham_Ip comparison generated 1300 (day 1), 2273 (day 3), 2694 (day

7), 2728 (day 14), and 242 (day 5) hits (Figure 2A). Notably, using strk_Ct as a control yielded a higher number of hits. This could result from the smaller inter-animal variation as strk_Ct samples were collected from the same set of mice that generated strk_Ip samples, while sham_Ip samples were from a different set of mice. Nearly 46% more hits were identified for day 1 when using strk_Ct as a control. This is likely due to “unchanged” strk_Ct proteome on day 1 in the contralateral area as aforementioned and/or an effect of craniotomy surgery in the

ipsilateral area of sham mice. With the fact that 71–80% of hits from strk_Ip and sham_Ip comparison were also identified as stroke hits when comparing against strk_Ct (Figure 2A), this study suggests that strk_Ct could serve as a control with the advantages of skipping sham animals and potentially having the smaller inter-animal variation, particularly for studies focused on the acute phase of stroke.

In this study, we focused on high-confidence protein hits generated by both above-described analyses with criteria of adjusted *p*-value <0.05 and the same direction of changes at each time point. This resulted in 1044 (day 1), 1631 (day 3), 2174 (day 7), 1941 (day 14), and 199 (day 28) proteins (represented as green bars in Figure 2A), yielding a total of 3625 proteins, hereafter referred to as “hits” (Table S2, SI). Notably, nearly half of the detected proteome responded to stroke, and most (57–76%) of the 3625 hits were down-regulated by stroke in the first four time points (Figure 2B).

Proteome Change Patterns and Associated Pathways

To understand the molecular pathways underlying the observed proteomic changes, we first performed clustering of the 3625 protein hits on expression means across 15 biological groups (strk_Ip, sham_Ip and strk_Ct at five time points) and then conducted enrichment analyses to determine pathways underlying different clusters. The *K*-mean clustering defined four distinct clusters representing 3.3% (cluster 1), 5.3% (cluster 2), 19.9% (cluster 3), and 71.5% (cluster 4) of the significantly changed proteome, respectively (Figure 3A). Cluster 1 showed a stroke-induced early peak of 119 proteins on day 3, and cluster 2 presented a later peak of 191 proteins on day 7, referred to as cluster-1_earlyUp and cluster-2_laterUp, respectively. Importantly, these two clusters together accounted for only ~8.6% of the protein hits, and they are all increased by stroke at the aforementioned time points compared to controls, with relatively large changes mostly greater than 2-fold. Cluster 3 also showed stroke-induced up-regulation in the expression of 722 proteins but with smaller amplitudes. This cluster contains proteins mostly peaked at day 7 with less than 1.5-fold, referred to as cluster-3_smUp. Cluster 4, composed of 2593 proteins, is the largest and the only one exhibiting stroke-induced down-regulation, mostly peaked on day 7 with relatively small magnitudes (<1.5-fold), referred to as cluster-4_smDw.

We next conducted pathway enrichment analysis using MetaCore (ClariVate Analytics) on each cluster. Of note, we also conducted the same analysis on all 7318 proteins to make sure the observed enrichment was not due to detection bias. More than 50 pathways were significantly enriched at FDR < 0.05 (Table S3 SI) for almost all clusters. We examined the top 10 pathways enriched from each cluster. As shown in Figure 3B, the most enriched pathways on cluster-1_earlyUp proteins are blood coagulation, immune responses via complement pathways, and plasmin signaling, reflecting early acute responses to stroke-induced diasthesis and edema. Cluster-2_laterUp proteins are enriched in both innate and adaptive immune responses. The later immune responses are mostly through B and T cell activation, resulting from phagocytosis, antigen presentation, and immunological synapse formation and involving IL-5 signaling. Differently, cluster-3_smUp proteins are mostly enriched in actin cytoskeleton remodeling, via Rho GTPases, and integrin-mediated cell adhesion and migration. In contrast to the three up-regulated clusters, the pathway enrichment of cluster-4_smDw proteins revealed that neurophysiological processes involving synaptic vesicle recycling,

AMPA receptor removal and delivery, and GABA-A receptor life cycle are the most enriched pathways, reflecting disrupted synaptic transmission and plasticity with both glutaminergic and GABAergic signaling being affected. Associated with neuronal activity and angiogenesis, respectively, the roles of CDK5 and angiotensin II signaling via beta-arrestin were also among the top enriched pathways. Interestingly, “ubiquinone metabolism” was also highly enriched, and 29 subunits of the NADH:ubiquinone oxidoreductase (respiratory complex I) were down-regulated by stroke (Table S3E, SI), signifying the dysfunction of the mitochondrial electron transport chain.

Collectively, clustering and pathway enrichment analyses revealed that the relatively large-scale changes in a small number of proteins are associated with acute and adaptive immune responses, suggesting their potential roles in the course of stroke via immune regulatory mechanisms.^{11,12} In contrast, the relatively smaller magnitude changes in the majority of the protein hits are linked to cytoskeleton remodeling (cluster-3_smUp) and synaptic signaling (cluster-4_smDw), which could be potentially relevant to spontaneous self-recovery from stroke-induced disruption.

Pharmacodynamic Biomarker Candidates

In addition to identifying the stroke-induced proteome changes and deciphering molecular pathways underlying AIS, we further explored the utilities of this dataset for drug discovery. We aimed to identify pharmacodynamic (PD) biomarker candidates from the 3625 protein hits by applying the following criteria: a PD biomarker candidate must be (1) a hit on at least two consecutive poststroke time points, (2) with a fold change (FC) ≥ 2 in stroke versus one or both controls on at least one of the consecutive time points, (3) with one of the consecutive time points in the first week, i.e., day 1, 3, or 7, and (4) identified by minimally two unique peptides. This resulted in a total of 309 proteins as top hits (referred to as “top hits” hereafter), of which 115, 106, and 88 proteins started changing on day 1, 3, and 7, respectively (Table 1, Figure S2, SI). Notably, all 309 top hits are up-regulated in stroke and mostly belonged to cluster-1_earlyUp or cluster-2_laterUp (Table S4, SI), likely reflecting the sustained and relatively large changes in inflammation and immune responses as observed in the pathway enrichment analyses.

To further facilitate selection of biomarker candidates, we used UniprotKB¹³ to determine whether these proteins have a secretion annotation. Promisingly, 182 of the 309 top hits are annotated as secreted proteins by their subcellular location and/or the presence of a signal peptide. Approximately 50% of these secreted proteins responded to stroke on day 1 and lasted up to a week, and ~40% responded on day 3 or 7 and lasted up to 2 or 4 weeks, covering a wide poststroke time range. Remarkably, more than 81% of the 182 secretion-annotated proteins are detected in human plasma according to the Plasma Proteome Database (PPD) (<http://www.plasmaproteomedatabase.org/>).¹⁴ Together, we propose that these proteins, particularly those secreted and/or present in human plasma (Table 1), could serve as PD biomarker candidates for acute, subacute, and chronic phases of stroke. It should be noted that while individual or a few protein hits could be further validated via complementary methodologies, a similar proteomic study using the serum or plasma from this mouse model would be an efficient approach to validate a large number of the candidates by correlating the protein changes between plasma and the brain cortex.

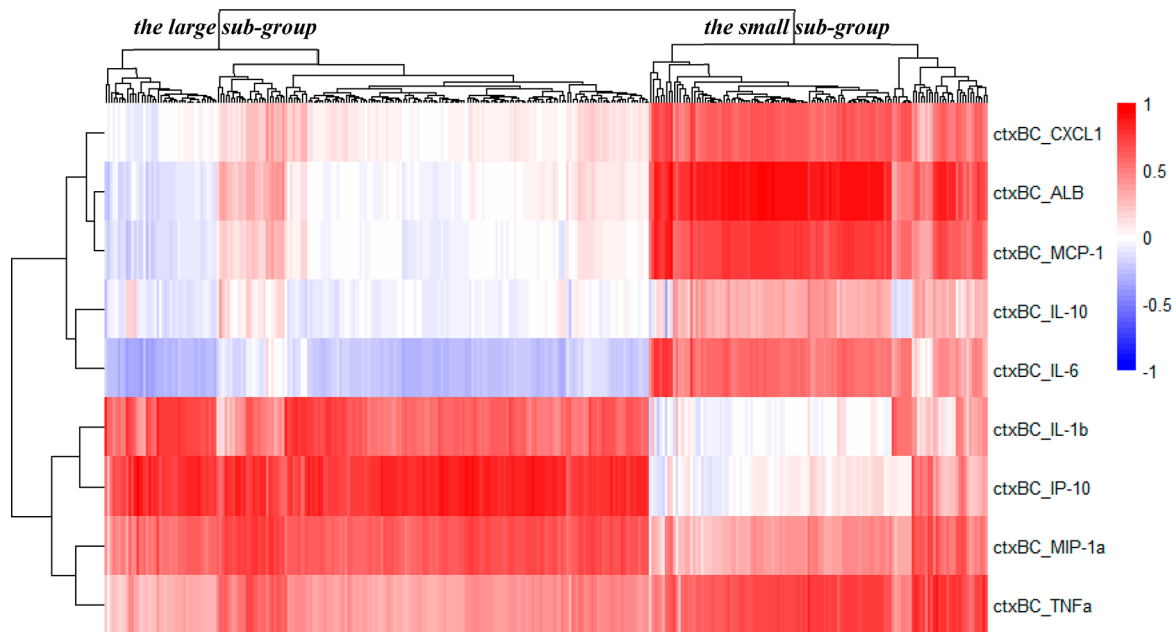


Figure 4. Association of the top hits to inflammatory markers. The heatmap shows pairwise correlation with a color gradient of blue (negative, $r = -1$) to red (positive, $r = 1$), indicating the strength. The dendrograms are hierarchical clustering on the Pearson correlation coefficients (r); x -axis, the 309 top hits from the proteomic analysis; y -axis, the eight cortical cytokines and albumin by biochemical analysis. The two big clusters of the top dendrogram are referred to as “the large subgroup” and “the small subgroup”, as described in text. Abbreviations: ctx, cortex; BC, biochemical method. Only strk_Ip and sham_Ip data were used in correlation analysis.

It is worth noting that some of these 309 top hits could be considered as therapeutic candidates as well, for example, proteins in the complement cascade. It is intriguing that many components of the complement cascade were among the 309 top hits and showed sustained changes for multiple time points. Previous work has shown that complement protein is deposited in the peri-infarct region in models of stroke and in post-mortem human tissue,^{15–19} which has been implicated in subsequent neuronal cell death. Indeed, genetic deletion of several complement proteins reduces infarct volume in the acute stages after stroke.^{17,19,20} More recently, pharmacological inhibition of the complement cascade, including when administered within 24 h after stroke, has been shown to reduce infarct size and promote behavioral recovery.^{18,21–23} These studies suggest that targeting complement proteins could be a potential neuroprotective strategy after stroke.

Association of the Top Hits to Inflammatory Markers

Preceding analyses revealed that cluster-1_earlyUp and/or cluster-2_laterUp proteins are highly enriched for inflammatory pathways, and the 309 top hits are mostly components of these two clusters. We thus sought to further determine the associations of these 309 top hits to known inflammatory markers in stroke, to identify potential PD biomarkers for AIS therapeutic approaches targeting inflammation. We quantified the levels of commonly used PD markers for inflammatory targets, namely, TNF α , IL-1 β , IL-6, IL-10, IP-10, CXCL1, MCP-1, and MIP-1 α , in the same brain cortex tissue analyzed in the proteomics study and evaluated their correlations to the 309 top hits. We additionally measured albumin (Alb) (Figure S3, SI) in the same brain tissues as a surrogate marker of the blood–brain barrier (BBB) leakage poststroke.

Pearson correlation analysis and hierarchical clustering on correlation coefficients (r) showed that the 309 top hits fell into two subgroups, one composed of about one-third (referred to as the small subgroup) and the other about two-thirds of the top

hits (referred to as the large subgroup), with each generally correlated to a different subset of cytokines (Figure 4). Most of the top hits in the small subgroup were highly correlated to Alb ($r > 0.6$), suggesting potential associations with BBB disruption, and correlated to a set of five cytokines (CXCL1, MCP-1, TNF α , IL-6, and MIP-1 α) at different strengths. In contrast, most of proteins in the large subgroup had no correlation to Alb ($|r| < 0.3$) and were highly correlated to IP-10, moderately to highly correlated to MIP-1 α and IL-1 β , and weakly to moderately negatively correlated to IL-6. Notably, most proteins in the small subgroup belong to cluster-1_earlyUp and most from the large subgroup are part of cluster-2_laterUp (Table S4, SI). This suggests that CXCL1, MCP-1, and TNF α represent acute responses, and IP-10, MIP-1 α and IL-1 β reflect the late response to stroke. Remarkably, at least 15 top hits overlap with “promising” stroke biomarker candidates (including MCP-1, TNF α , and IL-6) repeatedly investigated in other studies^{24,25} and/or clinical trials²⁶ for differentiating AIS from controls and/or subtypes of stroke. Eight of the 15 top hits, namely, Apoa1, Apoc1, Cd14, Egfr, Fn1, Orm1, Rbp4, and S100a9, belong to the small subgroup described above and 7 (Arg1, Cybb, Gbp4, Gfap, Iqgap1, Lag3, and Npl) to the large subgroup (Table S4, SI), indicating that they may play roles in immune responses at early or later stages poststroke, respectively. The fact that the top hits from this study recapitulate many promising stroke biomarkers not only further supports their potential as biomarkers but also endorses this study’s other novel top hits, with similar or stronger correlations to cytokines. For example, 10 proteins (Mag, Igfbp7, Lifr, C8b, C8a, Il1rap, Serpina3k, Serping1 and Serpinf2, Serpina3n) had the highest correlations to MCP-1 ($r > 0.77$) and were moderately to highly correlated to CXCL1, IL-6, TNF α , and Alb (Figure 5A), and a different set of 10 proteins (Fcer1g, Itgam, Cd68, Lgals9, Itgb5, Olfnl3, Ly86, Lgmn, Hexb, Fcgr1) had the highest correlations to IP-10 ($r > 0.85$) and were

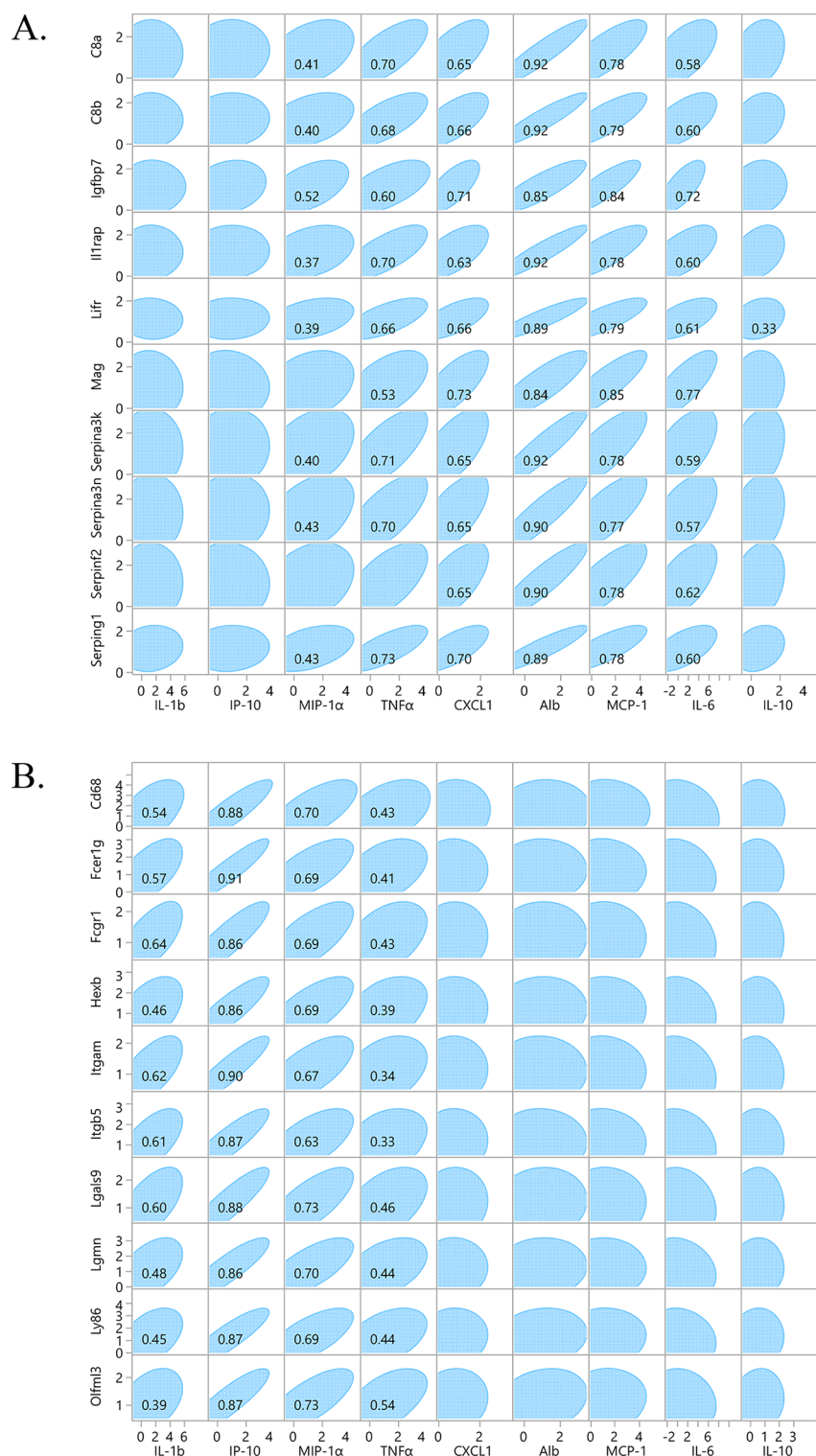


Figure 5. Exemplified differential correlation of top hits to cytokines and Alb. Example top hits (y-axis) from (A) the small subgroup or (B) the large subgroup (see Figure 4) were correlated, at cutoff $r \geq 0.33$ (r value shown), to different cytokines (x-axis) and/or Alb. Top hits that had the highest correlations to MCP-1 or IP-10 were selected for demonstration of the differentiated correlations to cytokines and Alb. The empty eclipses indicate no correlation ($r < 0.33$).

also correlated to MIP-1 α , IL-1 β , and TNF α , but not to Alb and the other four cytokines (Figure 5B).

The correlation analysis also divulged other intriguing observations. IL-6, an important mediator of inflammatory processes in the acute phase of stroke and reportedly a neurotrophic factor in the later phase,²⁷ was observed in this

study to positively or negatively correlate to cluster-1_earlyUp or a subset of cluster-2_laterUp proteins respectively, suggesting potential roles of some of cluster-2_laterUp top hits in neurogenesis. Additionally, proteins from both the small and large subgroups were, moderately and weakly, respectively, correlated to TNF α , a proinflammatory cytokine acting both

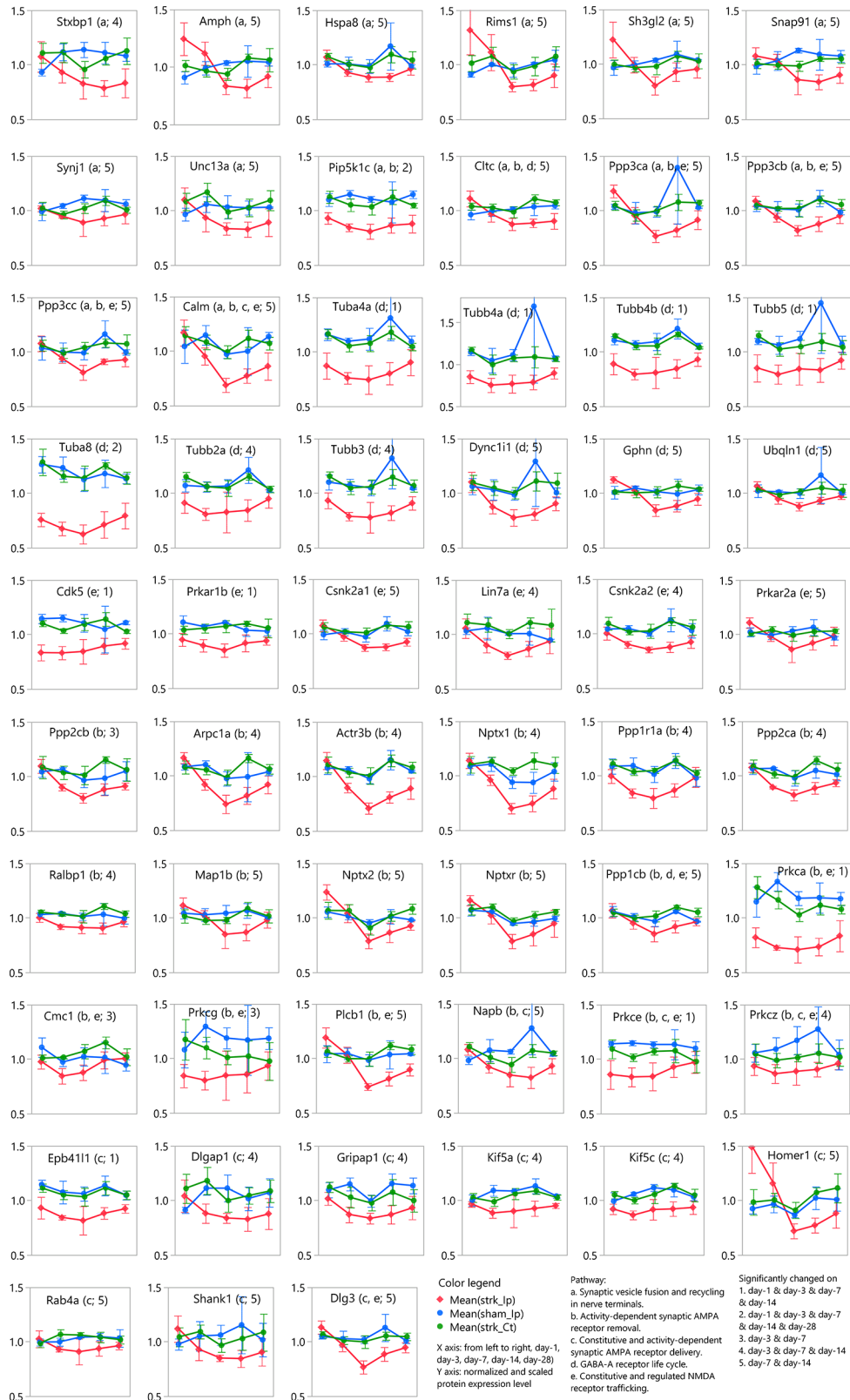


Figure 6. Profiles of 57 stroke-decreased proteins associated with top enriched neurophysiological process pathways. *x*-Axis, sample collection day poststroke. *y*-Axis, normalized protein expression level. Color legend: red, strk_Ip; blue, sham_Ip; and green, strk_Ct. The letters a–e in parentheses indicate the top enriched pathway in which the protein was involved: (a) synaptic vesicle fusion and recycling in nerve terminals (rank 1), (b) activity-dependent synaptic AMPA receptor removal (rank 2), (c) constitutive and activity-dependent synaptic AMPA receptor delivery (rank 6), (d) GABA-A receptor life cycle (rank 10), and (e) constitutive and regulated NMDA receptor trafficking (rank 12). The numbers 1–5 in parentheses indicate on which day the protein was significantly changed poststroke: (1) days 1, 3, 7, and 14, (2) days 1, 3, 7, 14, and 28, (3) days 3 and 7, (4) days 3, 7, and 14, (5) days 7 and 14.

locally in the brain and systemically in the periphery.²⁸ This may reflect that some of the top hits in the large subgroup are related to infiltration of peripheral immune cells. Furthermore, fewer proteins of the 309 top hits were correlated to IL-10, the only tested anti-inflammatory cytokine, suggesting that those IL-10-correlated top hits may have protective roles in stroke. Concertedly, the proteins highly correlated with cortical cytokines (Table S4, SI) could serve as PD biomarker candidates for stroke therapeutics modulating acute or chronic inflammation.

In contrast, the correlation analysis showed that the 309 top hits were not correlated to the measured cytokine levels in plasma, except for many of the small subgroup top hits that have weak negative correlations ($r = -0.33$ to -0.43) to plasma TNF α (Table S4, SI), possibly due to increased peripheral TNF α entering the brain. In addition, the cytokines measured in plasma were not correlated to their counterparts in brain, except for a weak correlation ($r = 0.36$) between brain and plasma IP-10 (Table S5, SI). These findings are consistent with the observation that the plasma levels of these cytokines are, in general, not good indicators of central nervous system inflammation in this DH-MCAO model.²⁹ Our results support that plasma levels of these cytokines do not have the desired specificity as stroke biomarkers.

Taken together, our analyses revealed that many of the stroke-changed top protein hits were highly correlated to one or more brain cytokines and could therefore be further validated as biomarkers for drug discovery aimed at early or later stages poststroke or other diseases with underlying inflammation.

Proteins Associated with Neurophysiological Processes

As the *K*-mean clustering analysis showed, the majority of stroke-changed proteins belong to cluster-3_smUp (approximately 20%) and cluster-4_smDw (over 70%), and none of these proteins met the criteria for the 309 top hits due to the small magnitudes of their changes. Cluster-3_smUp is enriched in proteins involved in cytoskeleton remodeling (RhoA, RhoC, Cdc42, Rac1, vinculin, different myosin subunits), as well as integrins (ITGB1, ITGA5) that participate in interactions with the extracellular matrix. We speculate that the changes in these proteins may underly pathological or adaptive changes in neurons to adjust to the damage in their microenvironment, by retracting damaged neurites or extending new ones. These responses would need to be characterized functionally to determine whether they are maladaptive or aimed at restoring homeostasis.

The pathway analysis for cluster-4_smDw showed that many neurophysiological processes were highly enriched for this cluster of proteins (Table S3E, SI) but not for the other three clusters (Table S3B–D, SI). Given that the initial phase of damage after stroke is followed by repair processes (e.g., increases in synaptic tone and axonal sprouting and synaptogenesis) aimed to restore normal neurological function, we speculate that the significantly changed proteins in the enriched neurophysiological processes could potentially play a role in recovery from stroke. We therefore had a closer look at the top five most enriched (ranked by FDR) neurophysiological process pathways for cluster-4_smDw, excluding those that were likely due to detection bias (see methods). The pathways we examined are synaptic vesicle fusion and recycling in nerve terminals (rank 1); activity-dependent synaptic AMPA receptor removal (rank 2); constitutive and activity-dependent synaptic AMPA receptor delivery (rank 6); GABA-A receptor life cycle (rank 10); and

constitutive and regulated NMDA receptor trafficking (rank 12). Among the protein hits involved in these pathways (Table S3E), we found 57 proteins that were decreased by stroke on at least 2 consecutive time points and identified by at least 2 unique peptides (Figure 6). Notably, most of the 57 proteins showed the strongest decrease at day 7, followed by a return to baseline, which might indicate potential recovery from stroke injury.

Stroke changed the abundance of many proteins related to the synaptic expression of neurotransmitter receptors, such as proteins in AMPA receptor removal and delivery, NMDA receptor trafficking, and GABA-A receptor life cycle. Included are many phosphatase subunits of PP2A, PP2B, and PP1B, components of clustering of AMPA-type glutamate receptors (Nptx1, Nptx2, Nptxr), multiple PKC subunits (Prkca, Prkce, Prkg, Prkcz), the Arp2/3 complex (Arpc1a), cytoskeleton remodeling (Actr3b, Gripap1, Kif5a, Kif5c) and postsynaptic components or those related (Dlgap1, Shank1), and protein kinases (Cdk5, Prkar1b, Prkar2a, Csnk2a1, Csnk2a2). Multiple α - and β -tubulin subunits (Tuba4a, Tuba8, Tubb2a, Tubb3, Tubb4a, Tubb4b, Tubb5), changed at different time points, were among 13 stroke-decreased proteins associated with the GABA-A receptor life cycle, indicating continued cytoskeleton remodeling via its major component microtubules. These changes in abundance of proteins related to AMPA and GABA-A receptors are consistent with recent attempts to target these receptor systems to promote stroke recovery. For example, potentiating the function of AMPA receptors and increasing their cell surface expression via the cytoskeletal protein CRMP2 promote the recovery of motor function in stroke models.^{30,31} Other components of AMPA receptor clustering or cytoskeleton remodeling identified here may serve as additional therapeutic targets. Similarly, inhibiting $\alpha 5$ -containing GABA receptors has been shown to promote sensorimotor recovery in mice.^{32–34}

Additionally, 14 proteins in synaptic vesicle fusion and recycling were significantly altered poststroke. These include calmodulin (Calm1), PP2B catalytic subunits (Ppp3ca, Ppp3cb, Ppp3cc), and PIP5K1-gamma (Pip5k1c), which are important upstream regulators of the transduction of intracellular Ca²⁺-mediated signals, indicating potentially disrupted neurotransmission and/or plasticity in stroke. Some of these proteins may also be potential therapeutic targets to promote recovery poststroke, and further work will be needed to validate them.

Taken together, our analysis of the cortex of stroke animals showed that synaptic function regulation via both glutaminergic and GABAergic receptor recycling is the most highly enriched underlying neurophysiological process, and the analysis generated a short list of protein candidates potentially valuable for neuronal-modulating therapeutics and poststroke recovery. It is worth pointing out that the changes we observed in the cortex likely reflect synaptic remodeling mechanisms encompassing motor and sensory projection neurons, transcallosal projections, and cortico-thalamic neurons.³⁵ To obtain a more complete picture of the recovery pathways, proteomic analysis of the thalamus and medulla, which are major neuronal relay stations, would need to be performed. Moreover, because many synaptic and plasticity events are regulated by phosphorylation, a phosphoproteomic analysis may provide additional insights about the mechanisms of poststroke recovery and identify new ways to promote recovery. Finally, it would be worthwhile to correlate the changes in protein abundance (or phosphorylation) to other measurements of poststroke recovery, such as an increase in electrophysiological activity or behavioral improvements.

CONCLUSION

The DH-MCAO model of stroke is well-suited for drug discovery research due to its reproducible detection of neurological deficits and molecular changes. To our knowledge, this is the first in-depth proteomic study using this model spanning a time course of 4 weeks poststroke. Our analysis reliably detected stroke-induced changes in the cortex in nearly half of the measured proteome and showed possible proteome recovery starting at day 14 poststroke. This study revealed that immune response pathways were enriched at both acute and chronic phases of stroke and reflected ~8.6% of the changed proteome, shedding new insights into the immune-regulatory mechanisms underlying stroke. The 309 top hits generated from this study, which overlapped with many promising stroke biomarkers, temporally responded to stroke at a relatively large-scale and differentially correlated to cortical cytokines and mostly secreted proteins, making them good biomarker candidates for immune-modulating and inflammation-targeting therapies. The study further divulged that decreases in protein abundances were relatively small, mostly peaked at 1 week poststroke, and subsequently returned to baseline, suggesting a process of spontaneous poststroke recovery. The identification of highly enriched neurophysiological processes and associated proteins offers new understandings in molecular mechanisms of AIS and should facilitate efforts to modulate synaptic receptor systems to promote neurological recovery from stroke.

ASSOCIATED CONTENT

Supporting Information

The Supporting Information is available free of charge at <https://pubs.acs.org/doi/10.1021/acs.jproteome.1c00259>.

Supplementary file 1 contains Supplementary Methods, tables, and figures, including Table S1 summarizing the TMT 10-plex design, Figure S1 showing differentiated proteomes in stroke and control samples, Figure S2 displaying temporal profiles of 309 top hits in stroke and control samples, and Figure S3 exhibiting Western blots of albumin in the brain cortex tissue samples (PDF)

Supplementary file 2 contains Table S2 listing 3625 proteins significantly changed by stroke, Table S3 summarizing the significantly enriched pathways underlying stroke-changed proteome, Table S4 cataloging 309 top hits and their correlation to cytokines and albumin, and Table S5 showing the correlation among eight cytokines and albumin (XLSX)

AUTHOR INFORMATION

Corresponding Authors

Linda C. Burkly – Genetic and Neurodevelopmental Disorders Research, Biogen, Cambridge, Massachusetts 02142, United States; Email: linda.burkly@biogen.com

Ru Wei – Chemical Biology and Proteomics, Biogen, Cambridge, Massachusetts 02142, United States; orcid.org/0000-0002-7646-9046; Email: ru.wei@biogen.com

Authors

Rong-Fang Gu – Chemical Biology and Proteomics, Biogen, Cambridge, Massachusetts 02142, United States

Terry Fang – Genetic and Neurodevelopmental Disorders Research, Biogen, Cambridge, Massachusetts 02142, United States

Ashley Nelson – Genetic and Neurodevelopmental Disorders Research, Biogen, Cambridge, Massachusetts 02142, United States

Stefka Gyoneva – Genetic and Neurodevelopmental Disorders Research, Biogen, Cambridge, Massachusetts 02142, United States

Benbo Gao – Chemical Biology and Proteomics, Biogen, Cambridge, Massachusetts 02142, United States

Joe Hedde – Genetic and Neurodevelopmental Disorders Research, Biogen, Cambridge, Massachusetts 02142, United States; Present Address: J.H.: Triplet Therapeutics, One Kendall Square, 1400W, Suite 14201, Cambridge, MA 02139.

Kate Henry – Genetic and Neurodevelopmental Disorders Research, Biogen, Cambridge, Massachusetts 02142, United States

Emily Peterson – Medicinal Chemistry, Biogen, Cambridge, Massachusetts 02142, United States

Complete contact information is available at:

<https://pubs.acs.org/10.1021/acs.jproteome.1c00259>

Author Contributions

L.C.B. and R.W. conceived the study; T.F., E.P., L.C.B., and R.W. directed the study; R.F.G., B.G., J.H., T.F., E.P., L.C.B., and R.W. designed the study. A.N. performed DH-MCAO surgery, collected the study samples, and drafted methods.; J.H. conducted the MSD assay (for cytokines) and W.B. (for Alb) and K.H. drafted the MSD and WB methods; R.F.G. performed proteomics sample analysis and data processing and drafted the methods; B.G. and R.W. performed proteomic data analysis, drafted methods, and prepared figures and tables; R.F.G., S.G., L.C.B., and R.W. wrote and edited the manuscript; and E.P. edited the manuscript. All authors reviewed and approved the manuscript.

Notes

The authors declare no competing financial interest.

The proteomics data are available in the PRIDE Archive with identifier PXD025077.

REFERENCES

- Chicheportiche, Y.; Bourdon, P. R.; Xu, H.; Hsu, Y. M.; Scott, H.; Hession, C.; Garcia, I.; Browning, J. L. TWEAK, a new secreted ligand in the tumor necrosis factor family that weakly induces apoptosis. *J. Biol. Chem.* **1997**, *272* (51), 32401–10. PMID: 9405449.
- Fluri, F.; Schuhmann, M. K.; Kleinschnitz, C. Animal models of ischemic stroke and their application in clinical research. *Drug Des., Dev. Ther.* **2015**, *9*, 3445–54. PMID: 26170628.
- Doyle, K. P.; Buckwalter, M. S. A mouse model of permanent focal ischemia: distal middle cerebral artery occlusion. *Methods Mol. Biol.* **2014**, *1135*, 103–10. PMID: 24510858.
- Doyle, K. P.; Fathali, N.; Siddiqui, M. R.; Buckwalter, M. S. Distal hypoxic stroke: a new mouse model of stroke with high throughput, low variability and a quantifiable functional deficit. *J. Neurosci. Methods* **2012**, *207* (1), 31–40. PMID: 22465679.
- Datta, A.; Jingru, Q.; Khor, T. H.; Teo, M. T.; Heese, K.; Sze, S. K. Quantitative neuroproteomics of an in vivo rodent model of focal cerebral ischemia/reperfusion injury reveals a temporal regulation of novel pathophysiological molecular markers. *J. Proteome Res.* **2011**, *10* (11), 5199–213. PMID: 21950801.
- Chen, J. H.; Kuo, H. C.; Lee, K. F.; Tsai, T. H. Global proteomic analysis of brain tissues in transient ischemia brain damage in rats. *Int. J. Mol. Sci.* **2015**, *16* (6), 11873–91. PMID: 26016499.
- Li, L.; Dong, L.; Xiao, Z.; He, W.; Zhao, J.; Pan, H.; Chu, B.; Cheng, J.; Wang, H. Integrated analysis of the proteome and

transcriptome in a MCAO mouse model revealed the molecular landscape during stroke progression. *J. Adv. Res.* **2020**, *24*, 13–27. PMID: 32181013.

(8) Agarwal, A.; Park, S.; Ha, S.; Kwon, J. S.; Khan, M. R.; Kang, B. G.; Dawson, T. M.; Dawson, V. L.; Andrabi, S. A.; Kang, S. U. Quantitative mass spectrometric analysis of the mouse cerebral cortex after ischemic stroke. *PLoS One* **2020**, *15* (4), e0231978. PMID: 32315348.

(9) Zheng, F.; Zhou, Y. T.; Zeng, Y. F.; Liu, T.; Yang, Z. Y.; Tang, T.; Luo, J. K.; Wang, Y. Proteomics Analysis of Brain Tissue in a Rat Model of Ischemic Stroke in the Acute Phase. *Front. Mol. Neurosci.* **2020**, *13*, 27. PMID: 32174813.

(10) Law, H. C.; Szeto, S. S.; Quan, Q.; Zhao, Y.; Zhang, Z.; Krakovska, O.; Lui, L. T.; Zheng, C.; Lee, S. M.; Siu, K. W.; Wang, Y.; Chu, I. K. Characterization of the Molecular Mechanisms Underlying the Chronic Phase of Stroke in a Cynomolgus Monkey Model of Induced Cerebral Ischemia. *J. Proteome Res.* **2017**, *16* (3), 1150–1166. PMID: 28102082.

(11) Chamorro, A.; Meisel, A.; Planas, A. M.; Urra, X.; van de Beek, D.; Veltkamp, R. The immunology of acute stroke. *Nat. Rev. Neurol.* **2012**, *8* (7), 401–10. PMID: 21738161.

(12) Iadecola, C.; Anrather, J. The immunology of stroke: from mechanisms to translation. *Nat. Med.* **2011**, *17* (7), 796–808. PMID: 21738161.

(13) The UniProt Consortium. UniProt: a worldwide hub of protein knowledge. *Nucleic Acids Res.* **2019**, *47* (D1), D506–D515. PMID: 30395287.

(14) Nanjappa, V.; Thomas, J. K.; Marimuthu, A.; Muthusamy, B.; Radhakrishnan, A.; Sharma, R.; Ahmad Khan, A.; Balakrishnan, L.; Sahasrabudhe, N. A.; Kumar, S.; Jhaveri, B. N.; Sheth, K. V.; Kumar Khatana, R.; Shaw, P. G.; Srikanth, S. M.; Mathur, P. P.; Shankar, S.; Nagaraja, D.; Christopher, R.; Mathivanan, S.; Raju, R.; Sirdeshmukh, R.; Chatterjee, A.; Simpson, R. J.; Harsha, H. C.; Pandey, A.; Prasad, T. S. Plasma Proteome Database as a resource for proteomics research: 2014 update. *Nucleic Acids Res.* **2014**, *42*, D959–D965. PMID: 24304897.

(15) Atkinson, C.; Zhu, H.; Qiao, F.; Varela, J. C.; Yu, J.; Song, H.; Kindy, M. S.; Tomlinson, S. Complement-dependent P-selectin expression and injury following ischemic stroke. *J. Immunol.* **2006**, *177* (10), 7266–74. PMID: 17082645.

(16) Mack, W. J.; Sughrie, M. E.; Ducruet, A. F.; Mocco, J.; Sosunov, S. A.; Hassid, B. G.; Silverberg, J. Z.; Ten, V. S.; Pinsky, D. J.; Connolly, E. S., Jr. Temporal pattern of C1q deposition after transient focal cerebral ischemia. *J. Neurosci. Res.* **2006**, *83* (5), 883–9. PMID: 16447284.

(17) Mocco, J.; Mack, W. J.; Ducruet, A. F.; Sosunov, S. A.; Sughrie, M. E.; Hassid, B. G.; Nair, M. N.; Laufer, I.; Komotar, R. J.; Claire, M.; Holland, H.; Pinsky, D. J.; Connolly, E. S., Jr. Complement component C3 mediates inflammatory injury following focal cerebral ischemia. *Circ. Res.* **2006**, *99* (2), 209–17. PMID: 16778128.

(18) Alawieh, A.; Langley, E. F.; Tomlinson, S. Targeted complement inhibition salvages stressed neurons and inhibits neuroinflammation after stroke in mice. *Sci. Transl. Med.* **2018**, *10* (441), eaao6459.

(19) Ducruet, A. F.; Sosunov, S. A.; Zacharia, B. E.; Gorski, J.; Yeh, M. L.; Derosa, P.; Cohen, G.; Gigante, P. R.; Connolly, E. S., Jr. The Neuroprotective Effect of Genetic Mannose-binding Lectin Deficiency is not Sustained in the Sub-acute Phase of Stroke. *Transl. Stroke Res.* **2011**, *2* (4), 588–99. PMID: 22505955.

(20) Soriano, S. G.; Coxon, A.; Wang, Y. F.; Frosch, M. P.; Lipton, S. A.; Hickey, P. R.; Mayadas, T. N. Mice deficient in Mac-1 (CD11b/CD18) are less susceptible to cerebral ischemia/reperfusion injury. *Stroke* **1999**, *30* (1), 134–9. PMID: 9880401.

(21) Alawieh, A.; Elvington, A.; Zhu, H.; Yu, J.; Kindy, M. S.; Atkinson, C.; Tomlinson, S. Modulation of post-stroke degenerative and regenerative processes and subacute protection by site-targeted inhibition of the alternative pathway of complement. *J. Neuroinflammation* **2015**, *12*, 247. PMID: 26714866.

(22) Alawieh, A.; Andersen, M.; Adkins, D. L.; Tomlinson, S. Acute Complement Inhibition Potentiates Neurorehabilitation and Enhances

tPA-Mediated Neuroprotection. *J. Neurosci.* **2018**, *38* (29), 6527–6545. PMID: 29921716.

(23) Alawieh, A. M.; Langley, E. F.; Feng, W.; Spiotta, A. M.; Tomlinson, S. Complement-Dependent Synaptic Uptake and Cognitive Decline after Stroke and Reperfusion Therapy. *J. Neurosci.* **2020**, *40* (20), 4042–4058. PMID: 32291326.

(24) Dagonnier, M.; Donnan, G. A.; Davis, S. M.; Dewey, H. M.; Howells, D. W. Acute Stroke Biomarkers: Are We There Yet? *Front Neurol* **2021**, *12*, 619721. PMID: 33633673.

(25) Bustamante, A.; Penalba, A.; Orset, C.; Azurmendi, L.; Llombart, V.; Simats, A.; Pecharroman, E.; Ventura, O.; Ribo, M.; Vivien, D.; Sanchez, J. C.; Montaner, J. Blood Biomarkers to Differentiate Ischemic and Hemorrhagic Strokes. *Neurology* **2021**, *96* (15), e1928–e1939. PMID: 33674361.

(26) Jickling, G. C.; Sharp, F. R. Biomarker panels in ischemic stroke. *Stroke* **2015**, *46* (3), 915–20. PMID: 25657186.

(27) Suzuki, S.; Tanaka, K.; Suzuki, N. Ambivalent aspects of interleukin-6 in cerebral ischemia: inflammatory versus neurotrophic aspects. *J. Cereb. Blood Flow Metab.* **2009**, *29* (3), 464–79. PMID: 19018268.

(28) Pawluc, H.; Wozniak, A.; Grzesk, G.; Kolodziejska, R.; Kozakiewicz, M.; Kopkowska, E.; Grzechowiak, E.; Kozera, G. The Role of Selected Pro-Inflammatory Cytokines in Pathogenesis of Ischemic Stroke. *Clin. Interventions Aging* **2020**, *15*, 469–484. PMID: 32273689.

(29) Doyle, K. P.; Quach, L. N.; Solé, M.; Axtell, R. C.; Nguyen, T. V.; Soler-Llavina, G. J.; Jurado, S.; Han, J.; Steinman, L.; Longo, F. M.; Schneider, J. A.; Malenka, R. C.; Buckwalter, M. S. B-lymphocyte-mediated delayed cognitive impairment following stroke. *J. Neurosci.* **2015**, *35* (5), 2133–45. PMID: 25653369.

(30) Clarkson, A. N.; Overman, J. J.; Zhong, S.; Mueller, R.; Lynch, G.; Carmichael, S. T. AMPA Receptor-Induced Local Brain-Derived Neurotrophic Factor Signaling Mediates Motor Recovery after Stroke. *J. Neurosci.* **2011**, *31* (10), 3766–75. PMID: 21389231. Correction: Clarkson, A. N.; et al. AMPA Receptor-Induced Local Brain-Derived Neurotrophic Factor Signaling Mediates Motor Recovery after Stroke. *J. Neurosci.* **2017**, *37* (42), 10252. PMID: 31305597.

(31) Abe, H.; Jitsuki, S.; Nakajima, W.; Murata, Y.; Jitsuki-Takahashi, A.; Katsuno, Y.; Tada, H.; Sano, A.; Suyama, K.; Mochizuki, N.; Komori, T.; Masuyama, H.; Okuda, T.; Goshima, Y.; Higo, N.; Takahashi, T. CRMP2-binding compound, edonergic maleate, accelerates motor function recovery from brain damage. *Science* **2018**, *360* (6384), 50–57. PMID: 29622647.

(32) Clarkson, A. N.; Huang, B. S.; Macisaac, S. E.; Mody, I.; Carmichael, S. T. Reducing excessive GABA-mediated tonic inhibition promotes functional recovery after stroke. *Nature* **2010**, *468* (7321), 305–9. PMID: 21048709.

(33) Wang, Y. C.; Dzyubenko, E.; Sanchez-Mendoza, E. H.; Sardari, M.; Silva de Carvalho, T.; Doepfner, T. R.; Kaltwasser, B.; Machado, P.; Kleinschnitz, C.; Bassetti, C. L.; Hermann, D. M. Postacute Delivery of GABAA alpha5 Antagonist Promotes Postischemic Neurological Recovery and Peri-infarct Brain Remodeling. *Stroke* **2018**, *49* (10), 2495–2503. PMID: 30355106.

(34) Lake, E. M.; Chaudhuri, J.; Thomason, L.; Janik, R.; Ganguly, M.; Brown, M.; McLaurin, J.; Corbett, D.; Stanis, G. J.; Stefanovic, B. The effects of delayed reduction of tonic inhibition on ischemic lesion and sensorimotor function. *J. Cereb. Blood Flow Metab.* **2015**, *35* (10), 1601–9. PMID: 25966952.

(35) Murphy, T. H.; Corbett, D. Plasticity during stroke recovery: from synapse to behavior. *Nat. Rev. Neurosci.* **2009**, *10* (12), 861–72. PMID: 19888284.